Hindawi Publishing Corporation
Journal of Quantum Chemistry
Volume 2014, Article ID 639851, 5 pages
http://dx.doi.org/10.1155/2014/639851

*Research Article*

# DFT Study on the Co-Xe Bond in the $HCo(CO)_3Xe$ Adduct

**Tamás Kégl**

*MTA-TKI Research Group for Selective Chemical Syntheses, Department of Inorganic Chemistry and János Szentágothai Research Center, University of Pécs, Ifjúság Útja 6, Pécs 7624, Hungary*

Correspondence should be addressed to Tamás Kégl; tkegl@gamma.ttk.pte.hu

Received 1 August 2013; Revised 1 October 2013; Accepted 15 October 2013; Published 2 January 2014

Academic Editor: Yinghong Sheng



The metal-xenon interaction has been studied in hydrido-cobalt-carbonyl complexes by means of density functional methods. The method of choice has been selected after testing various functionals including dispersion correction on the bond dissociation enthalpy of Xe in the $Cr(CO)_5Xe$ adduct. In general, the long range corrected versions of popular gradient-corrected functionals performed well. In particular, LC-mPWPW91 resulted in a perfect match with available experimental data; therefore this functional was selected for the computation of $HCo(CO)_3Xe$ adducts. For $HCo(CO)_3Xe$ two isomers have been located; the structure with $C_S$ symmetry has proved to be more stable by 5.3 kcal/mol than the $C_{3V}$ adduct in terms of free energy. The formation of $HCo(CO)_3Xe$ is, however, endergonic by 3.5 kcal/mol for the $C_S$ isomer.

## 1. Introduction

Hydroformylation of olefins is one of the most important applications of homogeneous catalysis in industry. The first precatalyst system containing $Co_2(CO)_8$ and $HCo(CO)_4$ was applied originally by Roelen [1]. This catalytic system is still in application predominantly for hydroformylation of higher olefins. According to Heck and Breslow [2] the initial step of the reaction is the dissociation of one of the CO ligands from $HCo(CO)_4$ resulting in $HCo(CO)_3$ as the active catalyst.

It is known that the rate of cobalt-catalyzed hydroformylation of olefins can be significantly reduced by the addition of a seemingly inert gas component such as $N_2$, Ar, or Xe to the reaction mixture [3–5]. The retarding effect can be explained by competitive coordination of the inert gas component, for example, the xenon to the catalytically active coordinatively unsaturated $HCo(CO)_3$ complex:

$$HCo(CO)_4 + Xe \longleftrightarrow HCo(CO)_3Xe + CO. \quad (1)$$

Among the few examples of transition metal, noble gas adducts and the $M(CO)_5$-Ng complexes (M = Group 6 metals; Ng = noble gas, such as argon, krypton, or xenon) are best examined. The experimental studies provided information about bond energies and infrared spectra [6, 7]; however, no structural information was obtained. The most comprehensive theoretical study on these types of complexes was completed by Ehlers et al. Optimized geometries and M-Ng bond energies were reported, which corresponded well with the experimental results [8].

Ono and Taketsugu investigated the binding of noble gas atoms to the coordinative highly unsaturated NiCO and CoCO species with density functional, multireference, and coupled-cluster methods [9, 10]. It was also shown that two Ng atoms can bind with Pt atom in linear geometry [11].

The aim of this work is to shed some light to the molecular and electronic structure and the bond dissociation energies of the isomers of $HCo(CO)_3Xe$. The secondary objective is a survey on the available density functional methods including dispersion correction by calculating the Cr-Xe bond strength in $Cr(CO)_5Xe$ and comparing it with the experimental value.

## 2. Computational Details

All the structures have been fully optimized without using symmetry constraints employing the Gaussian 09 suite program [12]. The def2-TZVP basis set [13] was utilized for every atom with the corresponding pseudopotential for Xe. The absence of negative eigenvalues has been confirmed by frequency calculations on the optimized geometries. Single

Table 1: Bond dissociation enthalpy (BDE) for the Cr-Xe bond in $Cr(CO)_5Xe$, including BSSE correction, as well as the computed Cr-Xe equilibrium distance.

| Functional | BDE (kcal/mol) | R(Cr-Xe) (Å) |
|---|---|---|
| B97D | 6.2 | 3.157 |
| VSXC | 15.7 | 3.066 |
| OLYP | 0 | 4.730 |
| LC-OLYP | 6.5 | 2.920 |
| M06L | 7.2 | 3.015 |
| BP86 | 4.5 | 2.968 |
| LC-BP86 | 10.3 | 2.800 |
| PBEPBE | 6.3 | 2.943 |
| LC-PBEPBE | 9.2 | 2.793 |
| mPWPW91 | 5.0 | 2.960 |
| LC-mPWPW91 | 9.0 | 2.801 |
| CAM-B3LYP | 4.2 | 3.019 |
| B98 | 4.0 | 3.021 |
| O3LYP | 0 | 3.015 |
| M06 | 7.5 | 2.957 |
| PBE0 | 6.0 | 2.922 |
| mPW1PW91 | 4.9 | 2.942 |
| Exp | 9.0 ± 1.0 | |

point calculations have been made with symmetry enabled on the respective point groups of each structure. The dissociation enthalpies for the metal-xenon bond have been counterpoise-corrected according to Boys and Bernardi [14]. NPA charges [15] and Wiberg bond indices (WBIs) on the NPA basis have been computed using the separate GENNBO 6.0 program because the NBO 3.1 version, implemented in Gaussian, results in highly erroneous natural atomic orbital occupancies. QTAIM (Quantum theory of atoms in molecules) calculations have been completed utilizing the AIMAll package [16]. For the charge decomposition analyses (CDA) the Multi.wfm program [17] has been employed.

## 3. Results and Discussion

The accurate determination of the strengths of Xe-metal bonds is a real challenge because most DFT methods lead us to more or less erroneous results. However, the introduction of dispersion (or long range) corrected functionals seems to overcome this problem. Therefore a set of dispersion corrected functionals have been selected, and their accuracies have been validated by computing the BDE of the Cr-Xe bond in $Cr(CO)_5Xe$, for which empirical data are available for comparison. Wells and Weitz reported 9.0 ± 1 kcal/mol by measuring the temperature dependence of the dissociation rate constant in gas phase [18]. The results are compiled in Table 1, along with the length of the Cr-Xe, which is anticipated to be indicative of the bond strength as well.

The set of functionals can be divided further into five groups: (i) original (uncorrected) GGA functionals frequently used for various studies, such as BP86, PBEPBE, OLYP, and mPW1PW91; (ii) their long range (LC) corrected versions developed by Ikura and coworkers [19]; (iii) standalone GGA functionals modified to handle weak interactions as well, such as B97D, VSXC, and M06L; (iv) hybrid functionals including dispersion correction, such as CAM-B3LYP and M06; and (v) uncorrected hybrid functionals.

In general, the hybrid functionals resulted in somewhat disappointing prediction for the BDE of $Cr(CO)_5Xe$. The O3LYP functional predicts no Cr-Xe interaction at all, whereas fairly small interaction energy is predicted by B98, CAM-B3LYP, and mPW1PW91. Somewhat better agreement with the experimental data has been achieved by PBE0. Among the hybrid functionals M06 provided the best result with a BDE being only 1.5 kcal/mol smaller than the experimental value.

Comparing the pure GGA functionals, it is remarkable that OLYP predicted no Cr-Xe interaction similar to its hybrid counterpart. Difference is, however, the Cr-Xe distance, which is also very large (4.730 Å). The inclusion of long range correction dramatically improves the accuracy increasing the BDE to 6.5 kcal/mol. Similar BDE was obtained by B97D, somewhat better by M06L. The remaining three uncorrected functionals also gave BDEs in this range; however, the LC correction for them resulted in spectacularly accurate results. LC-BP86 now somewhat overestimates the bond strength by 1.3 kcal/mol, whereas LC-PBEPBE and especially LC-mPWPW91 resulted in excellent agreement with the experimental BDE. Finally, the VSXC functional drastically overestimates the strength of the Cr-Xe interaction (15.7 kcal/mol) and, strangely, this is not reflected with the equilibrium Cr-Xe bond distance, which is over 3.0 Å. Thus, among the training set of functionals LC-mPWPW91 is selected for further studies and all the structural and electronical data provided below are obtained at the LC-mPWPW91/def2-TZVP level of theory.

The structure of $Cr(CO)_5Xe$ as well as that of the unsaturated $Cr(CO)_5Xe$ are depicted in Figure 1.

Upon coordination to chromium, the xenon atom loses some of its electron density, which is reflected by its positive NPA charge (0.230). As a light $\sigma$-donor, Xe also resulted in a minor elongation of the $Cr\text{-}C_{carbonyl}$ bond trans to Xe. On the other hand, the equatorial $Cr\text{-}C_{carbonyl}$ bonds have been contracted. The Cr-Xe distance is predicted to be 2.801 Å which is somewhat shorter than that reported by Ehlers and coworkers at the BP86 level [8].

Moving from the test complex to the cobalt-carbonyl complex, the structure of $HCo(CO)_3$ has been examined at the def2-TZVP level of theory. According to Huo et al. [20] two possible structures of singlet $HCo(CO)_3$ (with $C_{2v}$ and $C_{3v}$ symmetry) should be taken in account with an energy difference of 10.4 kcal/mol. The xenon coordination can take place on both structures resulting in a strongly distorted trigonal bipyramidal $C_s$ complex (denoted by $\mathbf{C_s}$) and a trigonal bipyramidal configuration in $C_{3v}$ symmetry ($\mathbf{C_{3v}}$), as illustrated in Scheme 1.

The geometries of the initial coordinatively unsaturated complexes $HCo(CO)_3$, as well as those for the adducts containing the coordinated xenon, are depicted in Figure 2.

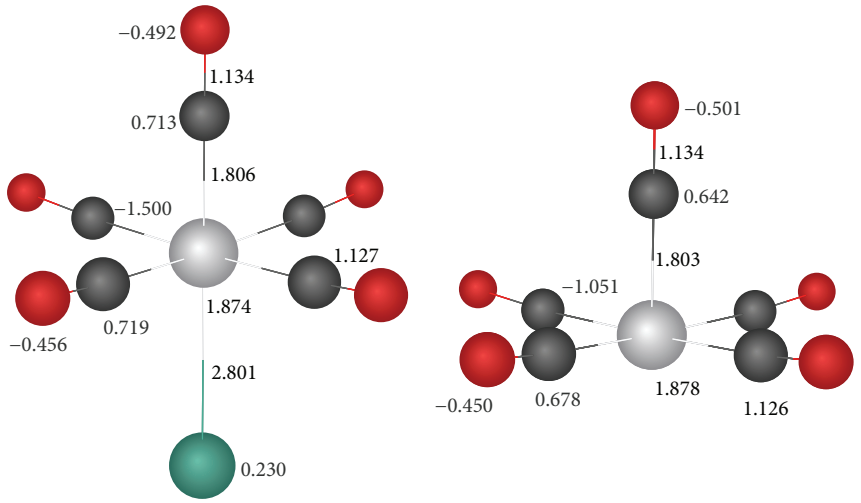


Figure 1: Optimized structure of $Cr(CO)_5Xe$ and $Cr(CO)_5$. Bond lengths are given in Å. The NPA charges are written in italics.

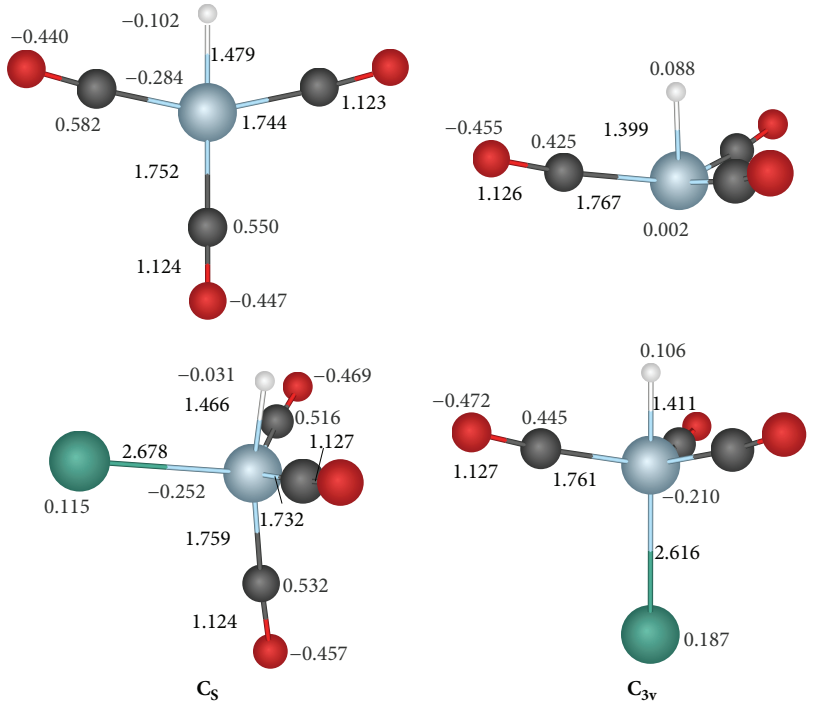


$C_S$ $C_{3v}$

Figure 2: Computed structures of $HCo(CO)_3$ and $HCo(CO)_3Xe$ isomers. Bond lengths are given in Å. The NPA charges are written in italics.

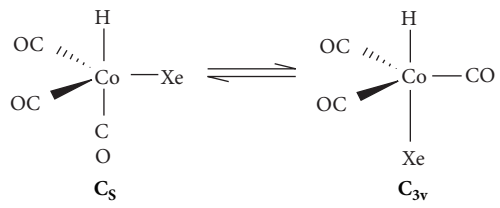


$C_S$ $C_{3v}$

Scheme 1

Unlike the B3LYP results, published by Beller et al., the LC-mPWPW91/def2-TZVP level resulted in a near planar structure with $C_s$ symmetry. Similar structure was reported by Ziegler and co-workers [21], albeit, with notably smaller bond angle for the carbonyl ligands cis to H through cobalt. The energy difference between the $C_{3v}$ and $C_s$ structures of $HCo(CO)_3$ is 10.9 kcal/mol, which is very close to that given by Beller [20].

The coordination of Xe to cobalt results in a slight change in geometry for the $\mathbf{C_s}$ structure with smaller equatorial C-Co-C bond angles. The free energy difference between $\mathbf{C_s}$ and $\mathbf{C_{3v}}$ is 5.3 kcal/mol in favor of the former isomer. Despite its lesser stability, the counterpoise-corrected BDE in $\mathbf{C_{3v}}$ is 11.1 kcal/mol, as opposed to that of $\mathbf{C_s}$ which is 5.7 kcal/mol. According to the free energy change of the adduct formation;

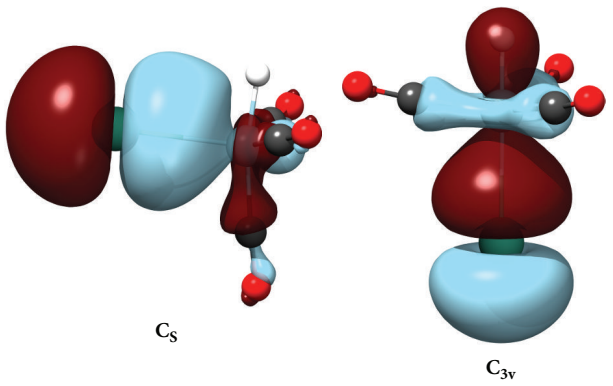


Figure 3: The HOMO-7 orbitals of $\mathbf{C_s}$ and $\mathbf{C_{3v}}$.

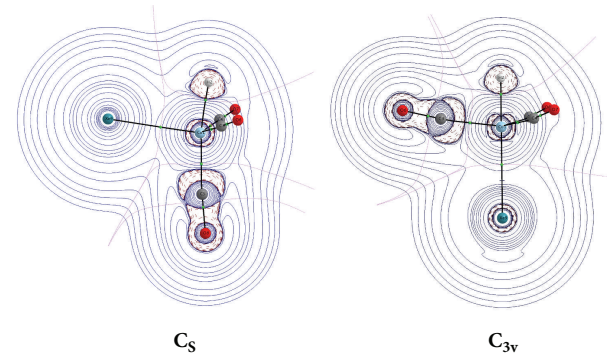


Figure 4: Contour line diagram of the Laplacian distribution $\nabla^2\rho(r)$ of the $HCo(CO)_3Xe$ isomers. Solid lines indicate charge depletion ($\nabla^2\rho(r) > 0$) and dashed lines indicate charge concentration ($\nabla^2\rho(r) < 0$).

however, the formation of both structures are endergonic, with $\Delta G$ = 3.5 and 8.8 kcal/mol for $\mathbf{C_s}$ and for $\mathbf{C_{3v}}$, respectively.

According to the NBO analysis the xenon atom is positively charged in both isomers of $HCo(CO)_3Xe$; that is, Xe loses some of its electron density when coordinating to the cobalt center. Its net charge increases from 0 to 0.115 and 0.187 in the case of $\mathbf{C_s}$ and $\mathbf{C_{3v}}$, respectively. As shown by CDA analysis, for the charge transfer mainly the binding HOMO-7 orbitals are responsible, which are shown in Figure 3. These are the only ones among the occupied orbitals where the p atomic orbitals of xenon ($p_x$ of $\mathbf{C_s}$ and $p_z$ of $\mathbf{C_{3v}}$) overlap significantly with the d orbitals of cobalt forming a $\sigma$-type interaction. The increase of natural charge is in strong correspondence with the decrease of the natural atomic orbital occupancy of the most interacting p orbital of xenon. The Wiberg bond indices (WBI) on the NAO basis of the Co-Xe bond (0.119 for $\mathbf{C_s}$ and 0.202 for $\mathbf{C_{3v}}$) are also in relationship with the natural charge of Xe. Thus, the greater degree of electron donation and hence the more positive partial charge of xenon, in the case of $\mathbf{C_{3v}}$, results in stronger bond to cobalt.

The nature of the Co-Xe bond was also examined by topological analysis of the electron density distribution evaluating the electron density in the Co-Xe bond critical point, as well as the delocalization index $\delta$(A,B), which is introduced by Bader and Stephens [22] and describes the number of electron pairs delocalized between two atomic basins. The $\delta$(A,B) is somewhat related to formal bond orders for an equally shared pair between two atoms in a polyatomic molecule; however, it is usually less than that due to delocalization over the other atoms in the molecule. For both structures bond path exists between Co and Xe, with a bond critical point. In contrast to the Wiberg bond indices, the electron density at the bond critical point is smaller for $\mathbf{C_{3v}}$ than that for $\mathbf{C_s}$, albeit, both values are rather small (0.0411 for $\mathbf{C_{3v}}$ and 0.0415 for $\mathbf{C_s}$). On the other hand, the delocalization index $\delta$(Co, Xe) results in the same order of bond strengths as WBI (0.482 for $\mathbf{C_{3v}}$ and 0.446 for $\mathbf{C_s}$). The Laplacian distribution of the $HCo(CO)_3Xe$ isomers are depicted in Figure 4. showing no significant distortion in the electron distribution around the xenon atom.

## 4. Conclusion

It can be concluded that xenon is able to coordinate to the coordinative unsaturated cobalt-catalyst under hydroformylation conditions; however, due to the endergonic formation of $HCo(CO)_3Xe$ it is probably not able to influence the rate of the reaction. The molecular orbital and the natural population analyses reveal that the Co-Xe bond may be characterized by the electron donation from one of the p atomic orbitals of xenon to cobalt. The survey on some commonly employed functionals show that in terms of BDE prediction the long range corrected LC-mPWPW91 functional very accurately describes the strength of the metal-xenon interaction.

## Conflict of Interests

The author declares that there is no conflict of interests regarding the publication of this paper.

## Acknowledgments

The author is thankful for the support of the Developing Competitiveness of Universities in the South Transdanubian Region (SROP-4.2.2/B-16-10/1-2010-0029) Project as well as the Supercomputer Center of the National Information Infrastructure Development (NIIF) Program.

## References

[1] O. Roelen, *Chemisches Zentralblatt*, vol. 927, 1953.

[2] R. F. Heck and D. S. Breslow, "The reaction of cobalt hydrotetracarbonyl with olefins," *Journal of the American Chemical Society*, vol. 83, no. 19, pp. 4023–4027, 1961.

[3] F. Piacenti, F. Calderazzo, M. Bianchi, L. Rosi, and P. Frediani, "Cobalt-catalyzed hydroformylation of olefins in the presence of additional "inert"gases," *Organometallics*, vol. 16, no. 20, pp. 4235–4236, 1997.

[4] L. Rosi, F. Piacenti, M. Bianchi, P. Frediani, and A. Salvini, "Cobalt-catalyzed hydroformylation of olefins in the presence of

xenon: Newexperimental evidence for metal-xenon adduct," *European Journal of Inorganic Chemistry*, vol. 1, pp. 67–68, 1999.

[5] M. Bianchi, P. Frediani, F. Piacenti, L. Rosi, and A. Salvini, "Influence of an additional gas on the hydroformylation and related reactions," *European Journal of Inorganic Chemistry*, no. 5, pp. 1155–1161, 2002.

[6] J. J. Turner, J. K. Burdett, R. N. Perutz, and M. Poliakoff, "Matrix photochemistry of metal carbonyls," *Pure and Applied Chemistry*, vol. 49, no. 3, pp. 271–285, 1977.

[7] X.-Z. Sun, M. W. George, S. G. Kazarian, S. M. Nikiforov, and M. Poliakoff, "Can organometallic noble gas compounds be observed in solution at room temperature? A time-resolved infrared (TRIR) and UV spectroscopic study of the photochemistry of $M(CO)_6$ (M = Cr, Mo, and W) in supercritical noble gas and $CO_2$ solution," *Journal of the American Chemical Society*, vol. 118, no. 43, pp. 10525–10532, 1996.

[8] A. W. Ehlers, G. Frenking, and E. J. Baerends, "Structure and bonding of the noble gas-metal carbonyl complexes M(CO)5-Ng (M = Cr, Mo, W and Ng = Ar, Kr, Xe)," *Organometallics*, vol. 16, no. 22, pp. 4896–4902, 1997.

[9] Y. Ono and T. Taketsugu, "Theoretical study of Ng-NiCO (Ng= Ar, Ne, He)," *Chemical Physics Letters*, vol. 385, no. 1-2, pp. 85–91, 2004.

[10] Y. Ono and T. Taketsugu, "Theoretical study of chemical binding of noble gas atom and transition metal complexes: Ng-NiCO, Ng-$NiN_2$, Ng-CoCO (Ng = He-Xe)," *Monatshefte für Chemie*, vol. 136, no. 6, pp. 1087–1106, 2005.

[11] Y. Ono, T. Taketsugu, and T. Noro, "Theoretical study of Pt-Ng and Ng-Pt-Ng(Ng=Ar,Kr,Xe)," *Journal of Chemical Physics*, vol. 123, Article ID 204321, 2005.

[12] Gaussian 09, Rev. C01, M. J. Frisch, G. W. Trucks et al., Gaussian, Inc., Wallingford, UK, 2009.

[13] F. Weigend and R. Ahlrichs, "Balanced basis sets of split valence, triple zeta valence and quadruple zeta valence quality for H to Rn: design and assessment of accuracy," *Physical Chemistry Chemical Physics*, vol. 7, pp. 3297–3305, 2005.

[14] S. F. Boys and F. Bernardi, "The calculation of small molecular interactions by the differences of separate total energies. Some procedures with reduced errors," *Molecular Physics*, vol. 19, pp. 553–566, 1970.

[15] A. E. Reed, L. A. Curtiss, and F. Weinhold, "Intermolecular interactions from a natural bond orbital, donor-acceptor viewpoint," *Chemical Reviews*, vol. 88, no. 6, pp. 899–926, 1988.

[16] AIMAll (Version 13. 05. 06) and T. A. Keith, *TK Gristmill Software*, Overland Park, Kan, USA, 2013.

[17] T. Lu and F. Chen, "Multiwfn: a multifunctional wavefunction analyzer," *Journal of Computational Chemistry*, vol. 33, pp. 580–592, 2012.

[18] J. R. Wels and E. Weitz, "Rare gas-metal carbonyl complexes: bonding of rare gas atoms to the Group VIB pentacarbonyls," *Journal of the American Chemical Society*, vol. 114, pp. 2783–2787, 1992.

[19] H. Ikura, T. Tsuneda, T. Yanai, and K. Hirao, "A long-range correction scheme for generalized-gradient-approximation exchange functionals," *Journal of Chemical Physics*, vol. 115, Article ID 3540, 2001.

[20] C. F. Huo, Y. W. Li, G. S. Wu, M. Beller, and H. Jiao, "Structures and energies of $[Co(CO)_n]^m$ ($m$ = 0, 1+, 1–) and $HCo(CO)_n$: density functional studies," *The Journal of Physical Chemistry A*, vol. 106, no. 50, pp. 12161–12169, 2002.

[21] T. Ziegler, L. Cavallo, and A. Bérces, "Density functional study on the electronic and molecular structure of the hydroformylation catalyst $HCo(CO)_3$," *Organometallics*, vol. 12, no. 9, pp. 3586–3593, 1993.

[22] F. W. Bader and M. E. Stephens, "Spatial localization of the electronic pair and number distributions in molecules," *Journal of the American Chemical Society*, vol. 97, no. 26, pp. 7391–7399, 1975.